Neuroendocrinology Letters Volume 47 No. 4 2026
ISSN: 0172-780X; ISSN-L: 0172-780X; Electronic/Online ISSN: 2354-4716
Web of Knowledge / Web of Science: Neuroendocrinol Lett
Pub Med / Medline: Neuro Endocrinol Lett

This work is licensed under Creative Common Attribution-NonCommercial-NoDerivatives 4.0 International (CC BY-NC-ND 4.0).
No permission to resale without signed publisher agreement.

ORIGINAL ARTICLE

OGTT-Evoked Neuromedin U Response and Gastrointestinal Pattern of Regional mRNA Expression in MSG-Induced Obesity in Rats

Ismail Hakki Akbudak[1], Fatih Altintas[2], Hasan Akca[2], Tunahan Anber[2], Melek Tunc-Ata[2], Vural Kucukatay[2]

1 Department of Internal Medicine, Faculty of Medicine, Pamukkale University, Denizli, Türkiye.
2 Department of Physiology, Faculty of Medicine, Pamukkale University, Denizli, Türkiye.

Correspondence to: Vural Kucukatay
Department of Physiology, Faculty of Medicine, Pamukkale University, Denizli, Türkiye
e-mail: vkucukatay@pau.edu.tr

Submitted: 2026-04-21 Accepted: 2026-06-19 Published online: 2026-06-19

Key words: **Decretin; Neuromedin U; monosodium glutamate; hypothalamic obesity; gastrointestinal tract**

Neuroendocrinol Lett 2026; **47**(4):204–214 **PMID:** 42460906 470406 © 2026 Neuroendocrinology Letters • **www.nel.edu**

Abstract

BACKGROUND: Neuromedin U (NMU) is a neuropeptide broadly expressed in the gastrointestinal (GI) tract and central nervous system (CNS), implicated in energy balance and glucose homeostasis. Recent studies have suggested that NMU may act as a "decretin" hormone by inhibiting glucose-stimulated insulin secretion (GSIS); however, in vivo findings remain inconclusive. This study evaluated plasma NMU responses during an oral glucose tolerance test (OGTT) and regional intestinal NMU expression in a monosodium glutamate (MSG)-induced hypothalamic obesity (MHO) model in rats.

METHODS: Thirty male Wistar rats were divided into control and MHO groups. MHO was induced by subcutaneous MSG injections during the neonatal period. After five months, metabolic parameters, oral glucose tolerance test (OGTT), plasma NMU levels, and NMU mRNA expression in the duodenum, jejunum, and ileum were analyzed using ELISA and RT-qPCR.

RESULTS: The MHO group exhibited elevated fasting glucose, decreased basal insulin levels, and increased abdominal adiposity compared to controls, indicating a metabolically obese phenotype in this model. Basal plasma NMU levels were similar between groups. At 60 minutes post-glucose load, plasma NMU decreased significantly relative to baseline in both groups, with no difference between MHO and control rats. Intestinal NMU expression followed a proximal-to-distal declining pattern, consistent with previous reports, and did not differ between MHO and control rats.

CONCLUSION: These findings suggest that NMU expression within the gastrointestinal tract remains regionally regulated and unaltered in experimental obesity. Furthermore, the significant decline in plasma NMU at 60 minutes is compatible with modulation during hyperglycemia but does not establish a causal role in glucose regulation. This pattern appears to be preserved in the MHO model despite metabolic dysfunction. Future studies employing receptor inhibition or NMU administration are warranted to elucidate its physiological role in insulin regulation.

INTRODUCTION

Obesity and metabolic syndrome (MetS) are global epidemics that significantly drive morbidity and mortality, with type 2 diabetes rising in both developed and developing nations (Hruby & Hu, 2015). About 537 million people currently live with diabetes, projected to reach 783 million by 2045 (Sun *et al.* 2022). While genetics contribute, lifestyle and environmental factors are the principal drivers. Gut and adipose tissues regulate metabolism via hormones that maintain energy balance (Wu *et al.* 2022), and adipose-derived mediators such as leptin, resistin, and TNF-α promote insulin resistance (Nieto-Vazquez *et al.* 2008). Gastrointestinal surgeries (e.g., gastric bypass, biliopancreatic diversion) are termed metabolic because they improve glucose control beyond weight loss (Fändriks, 2017), reducing body weight by ~60% and improving glucose tolerance by ~80% (Brolin, 2002), while lowering obesity-related risk and healthcare costs (Rubino & Gagner, 2002).

The foregut and hindgut hypotheses explain these benefits. The hindgut model proposes that rapid nutrient delivery to the distal intestine triggers signals improving glucose control (Campbell & Drucker, 2013), mediated by incretins such as GLP-1 and GIP (Nauck & Meier, 2016). The foregut model posits that excluding the duodenum/proximal jejunum suppresses signaling that impairs insulin action; thus, removing proximal intestine from nutrient flow may improve tolerance by inhibiting putative anti-incretins ("decretins") (Rubino *et al.* 2006).

This led to the idea that a proximally secreted, fasting-stimulated enteroendocrine decretin suppresses insulin production/secretion. Although none has been definitively identified, Neuromedin U (NMU) — a peptide expressed in gut and brain—has been proposed as a candidate (Alfa *et al.* 2015). Evidence is mixed: NMU suppressed glucose-stimulated insulin secretion in isolated perfused rat/human pancreas in vitro (Kaczmarek *et al.* 2006; Alfa *et al.* 2015), but several in vivo studies did not confirm this and instead suggested incretin-like actions (Peier *et al.* 2011; Ensho *et al.* 2019; Kuhre *et al.* 2019). The foregut-derived decretin concept predicts a proximally secreted factor suppressed by nutrient exposure that attenuates insulin release. Because oral glucose robustly engages enteroendocrine pathways, an OGTT is a physiological context in which to examine this hypothesis. Monitoring the time dependent dynamics of NMU throughout the OGTT allows us to determine whether circulating NMU is nutrient modulated in vivo and whether its pattern is compatible with a potential suppressive effect on the insulin response. The MSG-induced hypothalamic obesity model provides a suitable platform to assess whether these relationships are preserved under systemic metabolic dysfunction.

Therefore, we used a rat model of monosodium glutamate (MSG)-induced hypothalamic obesity (MHO). We hypothesized that obesity associated changes in β cell function and glycemia in MSG treated rats would be accompanied by changes in basal and glucose stimulated plasma NMU levels compared with controls. As a novel contribution, this study provides the first integrated characterization of both OGTT evoked NMU dynamics and regional intestinal NMU expression within the MSG induced hypothalamic obesity model. Our primary hypothesis was that MHO would alter circulating NMU responses to oral glucose, yielding a pattern compatible with a potential decretin like role, whereas our secondary hypothesis was that MHO would disrupt the canonical proximal to distal gradient of intestinal NMU expression. Accordingly, we descriptively assessed basal NMU concentrations, glucose induced NMU responses, and regional intestinal NMU mRNA expression, without manipulating NMU signaling directly. Specifically, because NMU is more highly expressed in proximal gut segments—stomach, duodenum, jejunum, proximal ileum (Mitchell *et al.* 2009)—we examined whether these regional NMU mRNA levels differ between MHO and controls.

MATERIAL AND METHODS

This in vivo experimental study is reported in accordance with the ARRIVE 2.0 guidelines for animal research. All procedures were conducted in compliance with institutional and national regulations for the care and use of laboratory animals.

Animals, housing and ethical approval

Thirty male Wistar albino rats, aged 3 months, were used in this study. Animals were provided by the Pamukkale University Animal Care Unit. All experimental procedures were approved by the Ethical Committee of Pamukkale University (approval number PAUHADYEK-2021/11), and animal care followed the Guide for the Care and Use of Laboratory Animals. Rats were housed in groups of four to five per stainless-steel cage under standard laboratory conditions (ambient temperature 24 ± 2 °C, relative humidity 50 ± 5%) with a 12-h light/12-h dark cycle. Animals had ad libitum access to standard chow and tap water throughout the study.

Group allocation and inclusion/exclusion criteria

The animals were randomly assigned into two equal groups: the Control group (n = 15) and the MSG-induced hypothalamic obesity (MHO) group (n = 15), using simple randomisation. Inclusion criteria required that the animals were healthy during the neonatal period, free of visible physical deformities, and fully adapted to laboratory conditions (12-hour light/dark cycle, 22 ± 2 °C). Pre-defined exclusion criteria were established to ensure data integrity and animal welfare. These included: (i) severe deterioration in general health or weight loss exceeding 20% of baseline

body weight (humane endpoints); (ii) technical complications during experimental procedures or sample collection (e.g., hemolysis of blood samples); and (iii) failure to develop the targeted obesity phenotype in the MSG/MHO group (non-responders), defined as a Lee index below the predefined threshold and/or lack of significant weight gain compared with controls. However, all animals in the present study successfully met the inclusion criteria and fulfilled the requirements of the targeted obesity model. No animals were excluded due to health issues, technical complications, or failure to develop obesity. Consequently, statistical analyses were performed on the entire cohort of 30 rats (Control group: n = 15; MHO group: n = 15).

Sample size and power calculation

An a priori power analysis was performed using G*Power software (version 3.1.9) to determine the minimum sample size required to detect statistically significant differences between the Control and MSG-treated (MHO) groups. Based on effect sizes reported in previous studies investigating MSG-induced obesity and gastrointestinal gene expression, the analysis was conducted with a two-sided α level of 0.05 and a target power (1−β) of 80%. The calculation indicated that a sample size of n = 15 rats per group (total N = 30) would provide adequate statistical power for the planned between-group comparisons, while accounting for potential biological variability.

Induction of MSG-induced hypothalamic obesity and experimental design

Animals were allocated into two experimental groups: control (C; n = 15) and monosodium glutamate–induced hypothalamic obesity (MHO; n = 15). MHO was induced during the neonatal period by subcutaneous injections of monosodium glutamate (MSG; 4 mg/g body weight, Sigma) on postnatal days 0, 2, 4, 6, 8, and 10. Control rats received an equivalent volume of isotonic saline (0.9% NaCl, 0.1 ml/g body weight) on the same postnatal days. Following neonatal treatment, animals were maintained under standard housing conditions for five months. Body weight was measured weekly from week 4 to week 16, and values were recorded to monitor growth and to support the characterization of the MHO phenotype. At the end of five months, metabolic characterization included oral glucose tolerance testing (OGTT), fasting plasma insulin, abdominal obesity indices, triglyceride (TG), total cholesterol (TC), high-density lipoprotein (HDL), low-density lipoprotein (LDL), Lee index, and Homeostasis Model Assessment of Insulin Resistance (HOMA-IR). A summary of the experimental design is presented in Figure 1.

Oral glucose tolerance test (OGTT) and insulin measurements

At the end of the fifth month, rats were fasted overnight for 12 h with free access to water. After the fasting period, a glucose solution (2 mg/g body weight) was administered by oral gavage. Tail vein blood samples were collected at 0 (baseline), 30, and 60 min to determine blood glucose and plasma insulin concentrations.

Blood glucose levels were measured immediately using a handheld glucometer (ACCU-CHEK Performa Nano). Plasma was separated by centrifugation, aliquoted, and stored until analysis. Plasma insulin concentrations at each time point (0, 30, and 60 min) were quantified using a commercial ELISA kit according to the manufacturer's instructions (E-EL-R2466; Elabscience). The OGTT procedure followed previously published protocols with minor adaptations (Nagy and Einwallner, 2018).

Plasma biochemical parameters and obesity indices

For biochemical analyses, rats were fasted for 12 h prior to blood sampling. Tail blood was collected, and plasma was obtained by centrifugation. Fasting plasma TG, TC, HDL, and LDL were measured using commercial enzymatic colorimetric kits (Elabscience, E-BC-K238,109; YL Biont, YLA0495RA, YLA0444RA), following the manufacturers' protocols. Basal and glucose-induced plasma neuromedin U (NMU) concentrations were determined at 0, 30, and 60 min of the OGTT using a specific ELISA kit (BTLab, E0719Ra).

At the end of the experimental period, abdominal adiposity was evaluated by dissecting and removing retroperitoneal and perigonadal fat pads. Each fat depot was carefully excised, blotted, and weighed; total abdominal fat was calculated as the sum of retroperitoneal and perigonadal fat masses and expressed relative to body weight (per 100 g). The Lee index, an anthropometric indicator of obesity in rodents, was calculated as body weight $^{1/3}$ (g) / naso-anal length (cm), as originally described by Bernardis and Patterson (1968) Insulin resistance was estimated using the HOMA-IR index, which was calculated as fasting plasma glucose (mmol/L) × fasting plasma insulin (mIU/L) / 22.5.

Real-time quantitative PCR (RT-qPCR) for intestinal NMU expression

To assess regional intestinal NMU expression, three gastrointestinal segments—duodenum, jejunum, and ileum—were collected from each experimental group at the end of the study. Approximately 100 mg of tissue from each segment was rapidly excised, rinsed in ice-cold saline, snap-frozen, and stored at −80 °C until RNA extraction. Total RNA was isolated using the Hibrizol Total RNA Mini Kit (HibriGen) according to the manufacturer's instructions. RNA concentration and purity were assessed spectrophotometrically using a NanoDrop™ 1000 (Thermo Scientific). Samples were stored at −80 °C until further processing. For cDNA

Copyright © 2026 Neuroendocrinology Letters ISSN 0172–780X • www.nel.edu

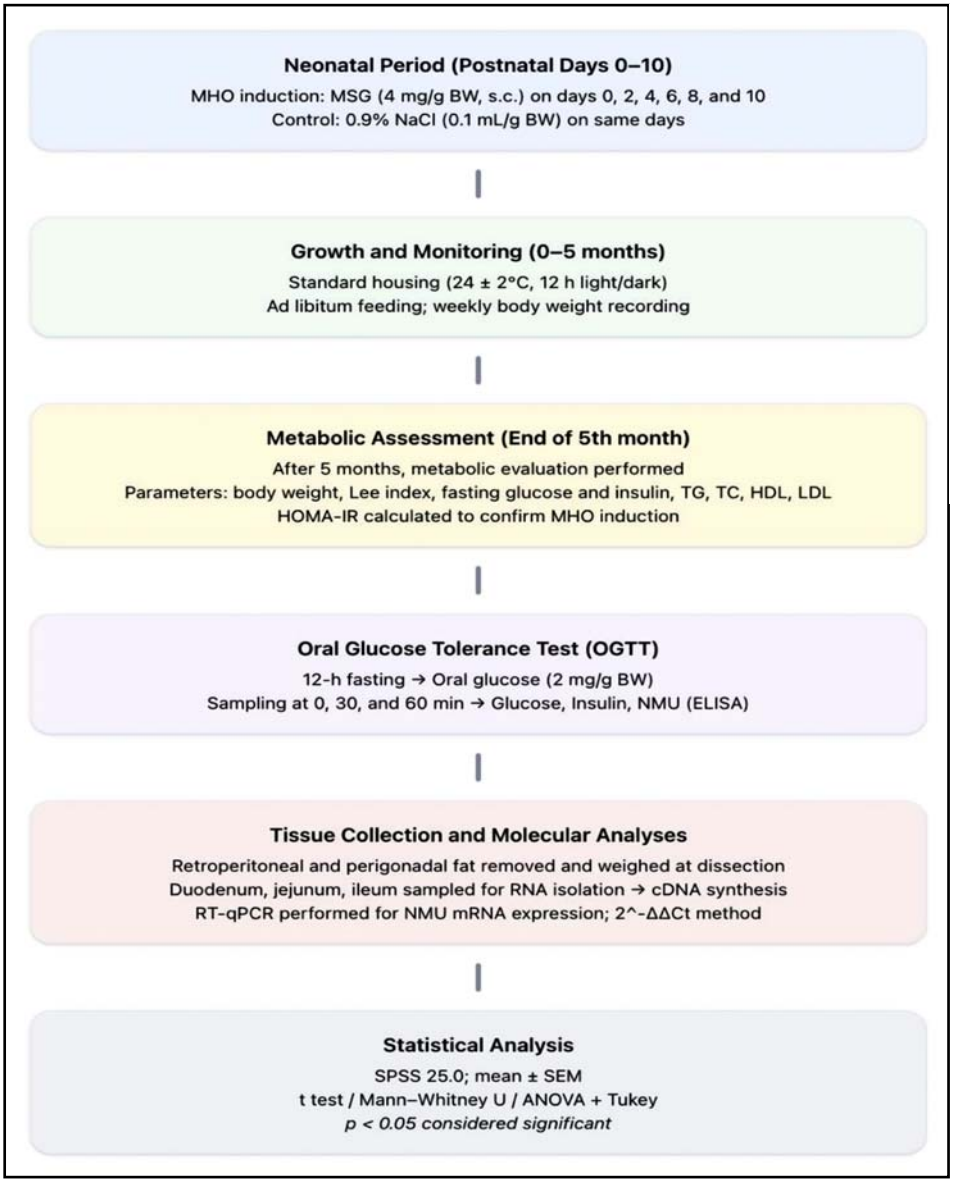

Fig. 1. Experimental design and timeline of MSG-induced hypothalamic obesity model. Schematic overview of neonatal treatment with monosodium glutamate (MSG) or saline, follow-up period, serial body-weight measurements, and terminal assessments at 5 months, including oral glucose tolerance test (OGTT), fasting biochemical measurements, abdominal fat sampling, and intestinal tissue collection. C, control; MHO, MSG-induced hypothalamic obesity.

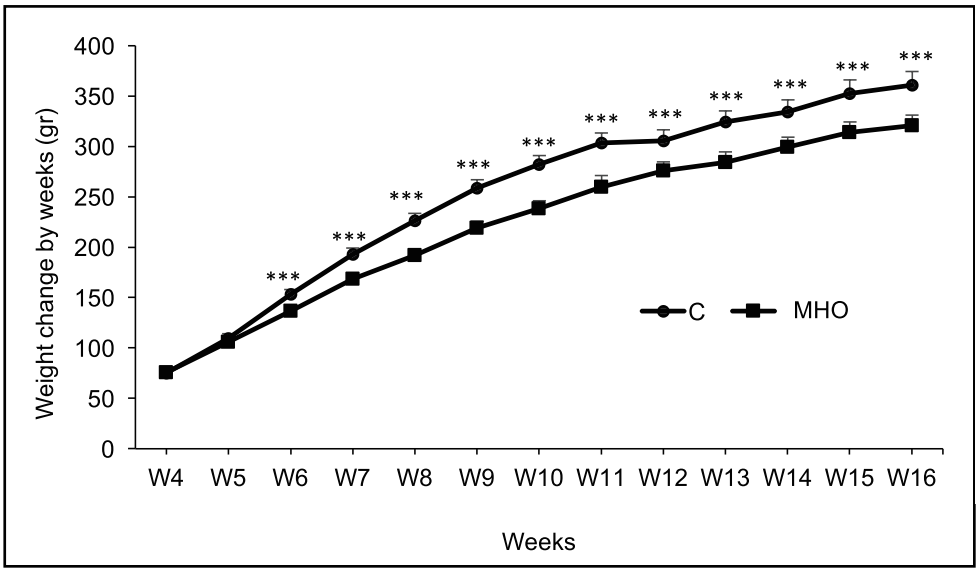

Fig. 2. Weekly body weight in control and MSG-induced hypothalamic obesity rats. Body weight (g) measured weekly from week 4 to week 16 in control (C) and MSG-induced hypothalamic obesity (MHO) groups. Values are mean ± SEM. *$p < 0.001$ vs C at corresponding time points.

synthesis, 1 µg of total RNA from each sample was reverse-transcribed using the OneScript® Plus cDNA Synthesis Kit (ABM) following the manufacturer's protocol. Quantitative real-time PCR (RT-qPCR) was performed using qPCR SybrMaster (Jena Bioscience) on a PikoReal Real-Time PCR System (Thermo Scientific). The thermal cycling protocol consisted of an initial enzyme activation step at 95 °C for 3 min, followed by 40 cycles of denaturation at 95 °C for 15 s and annealing/extension at 60 °C for 1 min, and a final melt-curve analysis for 20 min to verify amplicon specificity. All reactions were run in triplicate.

The expression of neuromedin U mRNA was normalized to the internal reference gene β-actin (actin beta). For each sample, the threshold cycle (Ct) of the target gene was first normalized to that of β-actin (ΔCt = Ct_target − Ct_actin). Relative expression levels were then calculated using the 2^−ΔΔCt method, where ΔΔCt = ΔCt_sample − ΔCt_control. Data are presented as fold change (relative quantification, RQ) compared with the control group. All biochemical, hormonal, and gene expression measurements were performed by investigators who were blinded to group allocation.

Statistical analysis

The experimental unit was the individual rat. Statistical analyses were performed using SPSS version 25.0 (IBM, Armonk, NY, USA). Continuous variables are expressed as mean ± standard error of the mean (SEM). The Shapiro–Wilk test was used to assess whether data conformed to a normal distribution. When parametric assumptions were met, differences between two independent groups were evaluated using the Student's t-test. For non-normally distributed data, the Mann–Whitney U test was applied. For comparisons involving more than two groups or multiple conditions, one-way analysis of variance (ANOVA) was used, followed by Tukey's post hoc test when appropriate. A two-sided p value < 0.05 was considered statistically significant for all analyses.

RESULTS

MSG-induced hypothalamic obesity (MHO) Results

Animals in groups C and MHO were weighed starting from week 4 until week 16 and weekly changes in body weight were monitored. It was found that the weights of animals in the MHO group were statistically significantly (p = 0.001) lower than those in the C group from week 6 (Figure 2). The Lee index, used as an indicator of obesity in rodents, was higher in the MHO group than in the C group but did not reach statistical significance (Figure 3). When fasting blood glucose levels were compared between the MHO and control (C) groups, the MHO group exhibited significantly higher fasting glucose concentrations than the control group (p = 0.0001) (Figure 4). The fasting blood insulin levels were significantly lower in the MHO group than in the C group (p = 0.01) (Figure 5). HOMA-IR, an index of insulin resistance, did not differ significantly between the MHO and control (C) groups (p = 0.3) (Figure 6). Lipid profiling showed higher LDL-C in the MHO group than in controls (p = 0.003 and p = 0.01, respectively), whereas HDL-C, triglycerides (TG), and total cholesterol (TC) did not differ significantly between groups (Figure 7). Retroperitoneal (Figure 8), perigonadal (Figure 9), and total abdominal fat (Figure 10) were all significantly higher in the MHO group than in controls (p = 0.0001), indicating greater abdominal adiposity despite lower overall body weight.

Glucose and insulin levels in response to OGTT

Following oral glucose administration (2 mg/g, gavage), blood glucose levels were higher in the MHO group than in controls at 0, 30, and 60 minutes (Figure 11a). In parallel, the insulin response to hyperglycemia was significantly blunted in the MHO group relative to controls at all time points (Figure 11b).

Neuromedin U response to OGTT

We evaluated the NMU response to the oral glucose tolerance test (OGTT) in MHO and control (C) rats.

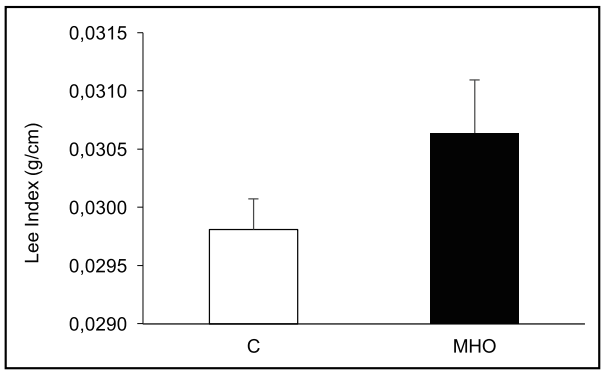

Fig. 3. Lee index as an indicator of obesity.
Lee index in control (C) and MSG-induced hypothalamic obesity (MHO) rats at 5 months. Values are mean ± SEM. Higher values indicate greater adiposity; the between-group difference did not reach statistical significance.

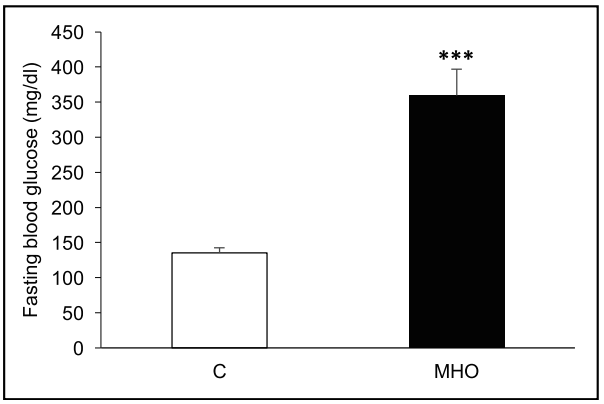

Fig. 4. Fasting blood glucose levels.
Fasting blood glucose (mmol/L) in control (C) and MSG-induced hypothalamic obesity (MHO) rats at 5 months. Values are mean ± SEM. *p < 0.001 vs C.

Copyright © 2026 Neuroendocrinology Letters ISSN 0172–780X • www.nel.edu

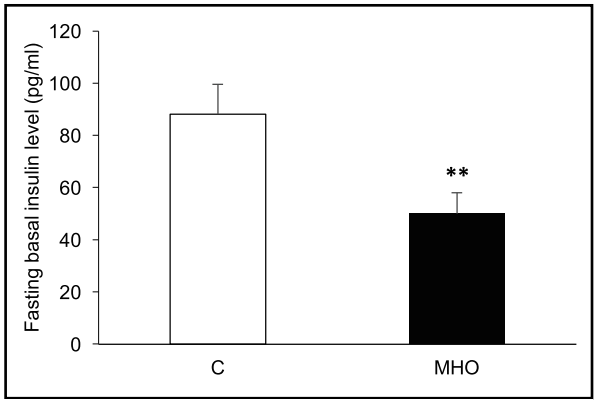

Fig. 5. Fasting plasma insulin levels.
Fasting plasma insulin (mIU/L) in control (C) and MSG-induced hypothalamic obesity (MHO) rats at 5 months. Values are mean ± SEM. *$p < 0.01$ vs C.

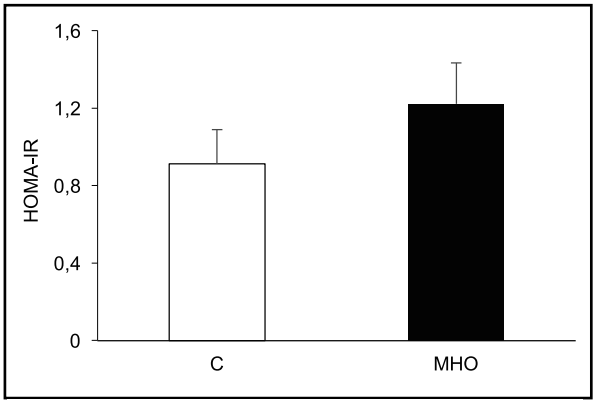

Fig. 6. HOMA-IR index.
Homeostasis model assessment of insulin resistance (HOMA-IR) in control (C) and MSG-induced hypothalamic obesity (MHO) rats. Values are mean ± SEM. No significant difference was observed between groups.

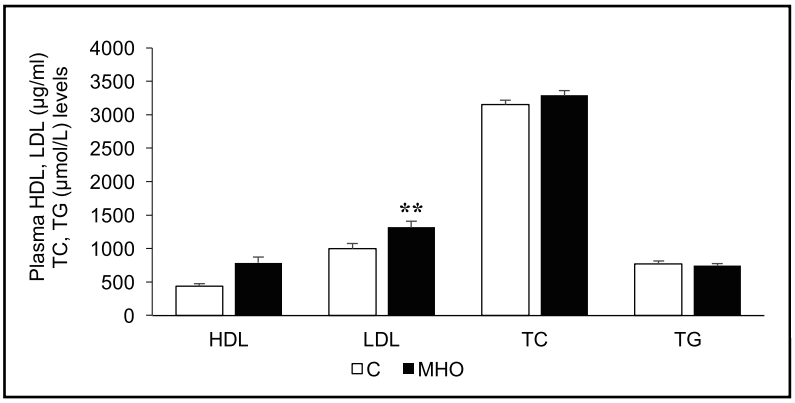

Fig. 7. Fasting lipid profile in control and MSG-treated rats.
Fasting plasma triglycerides (TG), total cholesterol (TC), high-density lipoprotein cholesterol (HDL-C), and low-density lipoprotein cholesterol (LDL-C) in control (C) and MSG-induced hypothalamic obesity (MHO) rats. Values are mean ± SEM. *$p < 0.01$ vs C for LDL-C; other parameters were not significantly different.

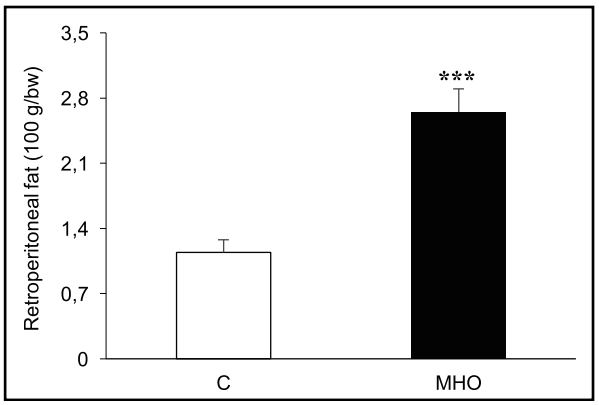

Fig. 8. Retroperitoneal fat mass.
Retroperitoneal fat mass expressed relative to body weight (g/100 g) in control (C) and MSG-induced ypothalamic obesity (MHO) rats. Values are mean ± SEM. *$p < 0.0001$ vs C.

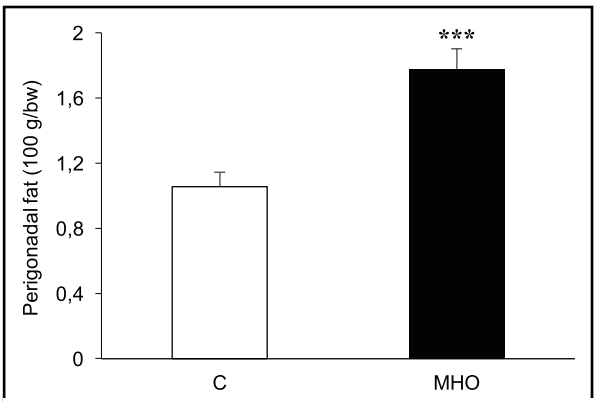

Fig. 9. Perigonadal fat mass.
Perigonadal fat mass expressed relative to body weight (g/100 g) in control (C) and MSG-induced hypothalamic obesity (MHO) rats. Values are mean ± SEM. *$p < 0.0001$ vs C.

Between group comparisons showed no differences in plasma NMU at baseline, 30, or 60 minutes. Within group analyses showed no change at 30 minutes versus baseline, whereas at 60 minutes plasma NMU levels were significantly reduced in both C and MHO groups (Figure 12), indicating a similar late phase decline in circulating NMU during the OGTT.

NMU relative gene expression results in duodenum, jejunum and distal intestine

In both groups, NMU protein expression declined progressively from proximal to distal gastrointestinal segments. The MHO group showed a pattern similar to controls (Figure 13).

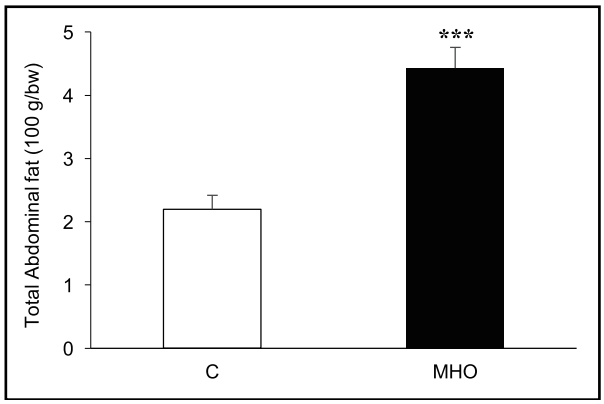

Fig. 10. Total abdominal fat mass.
Total abdominal fat mass (sum of retroperitoneal and perigonadal depots) expressed relative to body weight (g/100 g) in control (C) and MSG-induced hypothalamic obesity (MHO) rats. Values are mean ± SEM. *$p < 0.0001$ vs C.

DISCUSSION

The primary objective of this study was to evaluate the physiological response of Neuromedin U (NMU) to hyperglycemia and its gastrointestinal distribution in a monosodium glutamate (MSG)-induced hypothalamic obesity (MHO) model. We demonstrate that while the MHO model was successfully established with characteristic metabolic impairments—including abdominal adiposity and β-cell dysfunction—the physiological regulation of NMU remains preserved. Specifically, we observed a consistent suppression of plasma NMU during late-phase hyperglycemia, alongside a preserved proximal-to-distal gradient of NMU mRNA expression within the gastrointestinal tract in obese rats, mirroring the patterns observed in healthy controls.

Consistent with numerous studies using this model, we observed a marked reduction in weight gain in the MHO group relative to controls (C), beginning at week 6 and persisting through the five-month period, as shown by weekly body-weight measurements (Castrogiovanni *et al.* 2015; França *et al.* 2019; Rosa *et al.* 2016). Adiposity was assessed with the Lee index (Bernardis and Patterson, 1968; Rogers and Webb, 1980). Although MSG-treated rats showed a higher Lee index than controls, this difference was not statistically significant. We hypothesize that a larger sample size might align this parameter with studies in which the Lee index reached significance (Gaspar *et al.* 2016; Leguisamo *et al.* 2012; Lehnen *et al.* 2013). Considering body weight and Lee index together, the data indicate that, despite an increased obesity index in MHO rats, growth performance declined—consistent with prior reports (Caponi *et al.* 2013; Gaspar *et al.* 2016; Tunc-Ata *et al.* 2021). This phenotype is attributable to neonatal MSG exposure. Because the blood–brain barrier is immature during this period, MSG can enter the brain and exert toxic effects in the hypothalamus, particularly in arcuate-nucleus neurons (Olney, 1969). Damage to this nucleus reduces secretion of growth hormone–releasing hormone (GHRH) and impairs anterior pituitary growth hormone (GH) release (Maiter *et al.* 1991). Consequently, MSG-treated animals are smaller and leaner than controls. A complementary mechanism involves feeding regulation: the arcuate nucleus is central to appetite control, and MSG-treated animals are hypophagic with reduced hypothalamic neuropeptide Y (NPY) concentrations (Andreazzi *et al.* 2009; Husarova and Ostatnikova, 2013). Although MSG-based models are often described as hyperinsulinemic and normoglycemic—therefore suitable as prediabetic obese models (Hernández-Bautista *et al.* 2014; Pelantová *et al.* 2016)—our findings diverged: fasting glucose was significantly higher in MHO rats, whereas basal insulin was significantly lower than in controls. Notably, similar patterns have been reported: newborn male Wistar rats given MSG (4 g/kg/day, s.c.), versus saline controls, exhibited approximately two-fold higher fasting glucose after eight weeks (França *et al.* 2014; Nagata *et al.* 2006), and suppressed basal insulin has likewise been documented in MSG-treated groups (Yin *et al.* 2013).

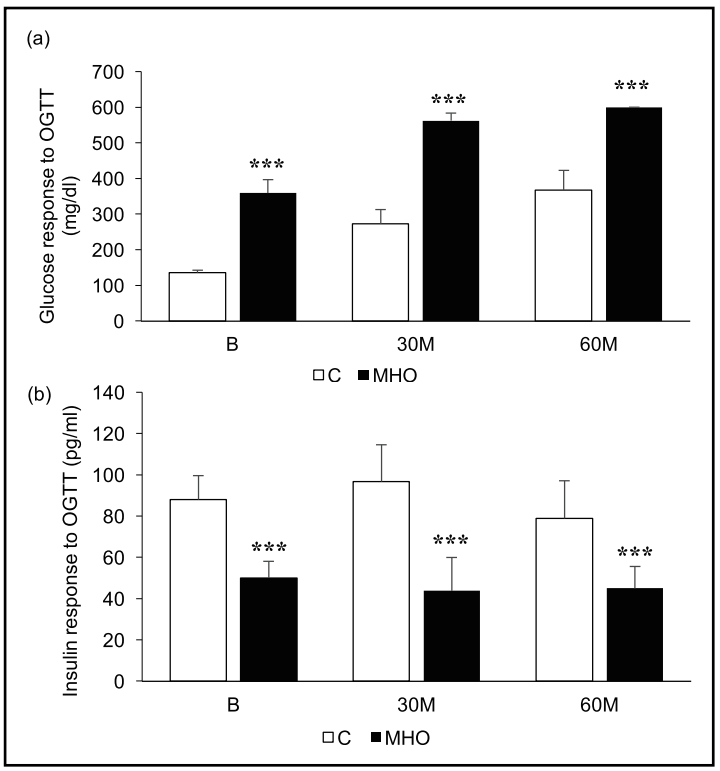

Fig. 11. Glucose and insulin responses to oral glucose tolerance test.
(a) Blood glucose (mmol/L) and (b) plasma insulin (mIU/L) at 0, 30, and 60 min during the OGTT in control (C) and MSG-induced hypothalamic obesity (MHO) rats. Values are mean ± SEM. *$p < 0.05$ vs C at corresponding time points.

Copyright © 2026 Neuroendocrinology Letters ISSN 0172–780X • www.nel.edu

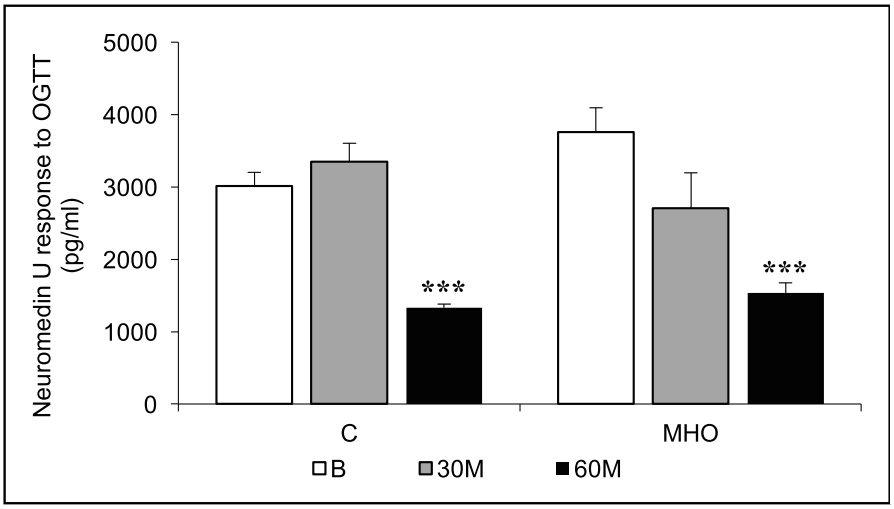

Fig. 12. Plasma neuromedin U levels during OGTT.
Plasma neuromedin U (NMU) concentrations at 0, 30, and 60 min during the OGTT in control (C) and MSG-induced hypothalamic obesity (MHO) rats. Values are mean ± SEM. *p < 0.05 vs baseline (0 min) within the same group.

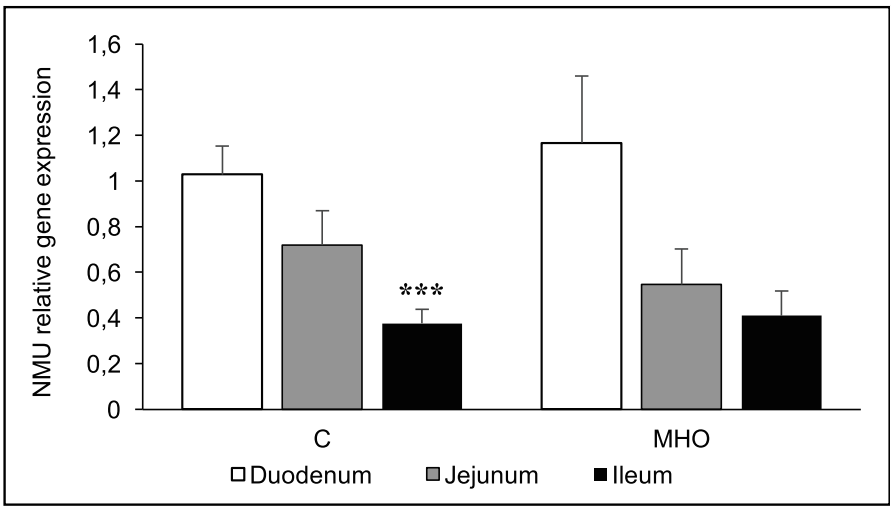

Fig. 13. Intestinal neuromedin U expression along the proximal–distal axis.
Relative neuromedin U (NMU) mRNA expression in duodenum, jejunum, and ileum of control (C) and MSG-induced hypothalamic obesity (MHO) rats, normalized to β-actin and expressed as fold change relative to the control duodenum. Values are mean ± SEM. NMU expression shows a proximal-to-distal decline in both groups, with no significant differences between C and MHO at corresponding segments.

The HOMA-IR index was used to evaluate insulin resistance. Classically, insulin resistance is accompanied by elevated insulin levels owing to compensatory hyperinsulinemia in response to hyperglycaemia. In contrast, the low insulin levels observed despite high blood glucose in our study more plausibly indicate impaired pancreatic β cell function or reduced β cell reserve rather than classical compensatory insulin resistance. Prior work with the same model has yielded mixed findings: some studies reported increased HOMA-IR (Sanches *et al.* 2016), whereas others—consistent with our data—found no significant change relative to healthy controls (Castrogiovanni *et al.* 2015).

A reduction in β cell reserve following MSG exposure may account for the absence of a significant HOMA IR difference between MSG treated and control groups. Indeed, multiple studies report that dietary MSG reduces pancreatic β cell mass in adult mice, mirroring the loss observed after neonatal MSG administration (Boonnate *et al.* 2015; Nakayama *et al.* 2003; Yin *et al.* 2013). Thus, a decline in β cell capacity in the face of rising glycaemia is a plausible explanation for the attenuated insulin response, although this remains inferential because β cell mass was not directly quantified in our study. Although the mechanism of MSG induced β cell loss remains unresolved, oxidative stress within β cells has been proposed as a contributing pathway (Boonnate *et al.* 2015; Di Cairano *et al.* 2011).

In the OGTT, oral glucose (2 mg/g) increased blood glucose at 30 and 60 minutes in both groups; however, the rise reached statistical significance only in the MHO group. The insulin response was significantly suppressed in MHO rats at both time points. Although controls exhibited higher plasma insulin than MHO at all time points, they still failed to mount an adequate response to the glycemic load. The hyperglycemia observed in controls—likely reflecting an insufficient insulin response—may be attributable to anesthesia. Prior reports show that anesthetics disrupt glycemic regulation and elevate blood glucose in experimental animals (Windeløv *et al.* 2016). This aligns with the hyperglycemia and hypoinsulinemia observed here and is mechanistically consistent with anesthetic activation of ATP-sensitive K^+ channels in β-cells, which inhibits insulin release (Zuurbier *et al.* 2008).

Literature regarding the lipid profile in the MHO model is heterogeneous, with some studies reporting broad dyslipidemia while others observe only specific alterations (Leguisamo *et al.* 2012; Sanches *et al.* 2016). In our study, although Total Cholesterol (TC), Triglyceride (TG), and HDL levels remained unchanged, we observed a specific and significant elevation in LDL cholesterol in the MHO group compared to controls. This isolated increase in LDL is physiologically relevant, as it indicates a shift toward an atherogenic lipid profile even in the absence of overt hypertriglyceridemia. While the variability in lipid outcomes across studies likely stems from differences in MSG dosage, administration protocols, or study duration, our data suggest that neonatal MSG exposure compromises lipid metabolism, specifically impairing LDL homeostasis.

Studies on rats administered MSG during the neonatal stage consistently revealed a pattern of abdominal obesity despite the overall underweight status. This condition, known as metabolic obesity, is characterized by excessive fat accumulation in the abdominal area. In our investigation, we examined abdominal obesity by collecting perigonadal and retroperitoneal fats from the MHO group and comparing them to those from the control group. Our findings, in line with existing research, demonstrate a significant increase in abdominal fat in the MHO group (Castrogiovanni *et al.* 2015; Lehnen *et al.* 2013; Sanches *et al.* 2016). It is known that this phenomenon results from MSG injection-induced damage to the arcuate nucleus, which disrupts the energy balance and lipid metabolism in animals (Brosnan *et al.* 2014). A previous research has shown that MSG administration leads to excessive fat accumulation in adipose tissue due to an imbalance between lipogenesis and lipolysis (Dolnikoff *et al.* 2001). In our study, administration of MSG to neonatal rats increased intra-abdominal visceral adipose tissue as a consequence of neuroendocrine disruption, presenting a typical obesity model.

The role of NMU in glucose homeostasis has been investigated from multiple angles (Peier *et al.* 2011). For example, expression of NMU and NMUR1 has been demonstrated in rat pancreatic islets, in mouse β-cells, and in the β-cell–derived MIN6-K8 line; moreover, NMU applied to these cells—as well as to isolated human islets—has been reported to suppress insulin secretion (Alfa *et al.* 2015; Teranishi and Hanada, 2021). In addition to these in vitro findings, in vivo studies have also reported that NMU suppresses insulin secretion (Zhang *et al.* 2017). Overall, it has been proposed that NMU, acting via NMUR1 receptors, attenuates glucose-stimulated insulin secretion (GSIS) through autocrine or paracrine mechanisms and may therefore function as a "decretin" hormone (Peier *et al.* 2011). Conversely, opposing results have been published: subcutaneous NMU administration has been shown to increase insulin secretion—likely via GLP-1—and NMU knockout in mice had no effect on plasma glucose or insulin levels, with or without glucose administration (Ensho *et al.* 2019).

In our study, plasma NMU levels did not differ between the control (C) and MHO groups at baseline or 30 minutes after the OGTT. However, at 60 minutes, plasma NMU levels significantly decreased relative to baseline in both groups. We interpret this physiological decline as a pattern that is compatible with, but does not prove, the decretin hypothesis. If NMU functions as a negative regulator of insulin secretion, circulating levels might be expected to fall during hyperglycemia; our findings are consistent with this possibility but remain purely correlative. Thus, the reduction in NMU at 60 minutes should be regarded as hypothesis generating for a potential decretin like role, rather than as definitive evidence. Notably, this dynamic response was preserved in the MHO group despite their metabolic impairments, suggesting that while MSG-induced lesions compromise β-cell mass, the systemic signaling pathway responsible for downregulating NMU during glucose excursion remains intact.

NMU (neuromedin U) is a neuropeptide with a broad tissue distribution in humans and rats. It is found predominantly in the gastrointestinal (GI) tract and the central nervous system (CNS), the two principal sites in which NMU expression is enriched (Teranishi and Hanada, 2021). In human studies, NMU immunoreactivity is detectable throughout the GI tract from the stomach to the rectum, with the highest levels in the jejunum (Austin *et al.* 1995). Taken together, these findings indicate a general pattern in which NMU expression declines from proximal to distal intestinal segments (e.g., from duodenum/jejunum toward ileum).

Nevertheless, despite this well-characterized proximal–distal distribution, direct and quantitative data on how this pattern changes in experimental obesity models (e.g., high-fat diet/diet-induced obesity [DIO], monosodium glutamate [MSG] models) remain limited. In a recent clinical study, duodenal NMU expression did not differ between individuals with obesity and/or type 2 diabetes (T2D) and healthy controls. Against this backdrop, another objective of our study was to compare the basal GI distribution pattern of NMU in a previously unexamined experimental obesity model with that of a control group. Our results, consistent with the literature, demonstrated that NMU expression decreases from the proximal to the distal GI tract (duodenum to ileum). We further found that this declining pattern does not differ from controls in our experimental obesity model. To our knowledge, these findings provide the first quantitative evidence that the proximal-to-distal gradient of NMU expression reported in individuals with obesity and/or type 2 diabetes is also maintained in an MSG-induced experimental obesity model. This overall perspective suggests that NMU possesses a regionally organized

Copyright © 2026 Neuroendocrinology Letters ISSN 0172–780X • www.nel.edu

expression profile within the gastrointestinal (GI) tract and that, despite changes in metabolic status (at least in our model), this fundamental regional pattern remains preserved.

The limitations of our study can be listed as follows. Our primary aim was descriptive physiology, not mechanism discovery; accordingly, the constraints below reflect the scope of our design.

1) The independence of NMU expression and plasma levels from insulin related measures constrains the ability of the study to draw conclusions regarding the role of NMU as a decretin. Without experiments specifically designed to assess the impact of NMU on insulin secretion—such as NMU administration in vitro or in vivo, or knockout studies—no definitive conclusion can be derived from the current data concerning NMU's role as a decretin; our findings are therefore limited to a descriptive characterization of NMU behavior during OGTT and along the gastrointestinal tract.. Therefore, all interpretations regarding a decretin-like function of NMU in this study should be considered hypothesis-generating rather than confirmatory. Nonetheless, these negative results are still important for the decretin hypothesis.
2) Another limitation is that plasma levels were measured from blood taken from the systemic circulation. As studies have reported that NMU is rapidly degraded in the systemic circulation (Takayama *et al.* 2016), our results on plasma NMU levels measured systemically make this finding difficult to interpret. Therefore, we think that measurement of NMU response to OGTT in blood obtained from the portal circulation will yield more accurate results.
3) Third, the use of anesthesia may have contributed to hyperglycemia and hypoinsulinemia during the OGTT in both groups, potentially blunting between group differences in glucose–insulin dynamics.

In conclusion, this study provides the first quantitative evidence that the systemic NMU response to glucose load and its regional intestinal expression are resilient to the neuroendocrine disruptions characterizing the MHO model. Rather than exhibiting a distinct obesity-associated defect, the NMU system in this model shows a similar late-phase decline during hyperglycemia and a preserved regional intestinal expression pattern, regardless of metabolic status. Future research should move beyond descriptive profiling to functional interventions, such as specific receptor blockade or direct NMU administration, to map its mechanistic contribution to insulin regulation and β-cell compensation in metabolic disorders.

CREDIT AUTHORSHIP CONTRIBUTION STATEMENT

All authors contributed to the study conception and design. **Ismail Hakki Akbudak**: Writing – Original Draft, Visualization **Fatih Altintas**: Conceptualization, Methodology, Investigation **Hasan Akca**: Validation, Formal analysis **Tunahan Anber**: Methodology, Formal analysis **Melek Tunc-Ata**: Methodology **Vural Kucukatay**: Resources, Writing - Review & Editing, Supervision, Project administration, Funding acquisition. All authors read and approved of the final manuscript.

DECLARATION OF COMPETING INTEREST

The authors declare that they have no known competing financial interests or personal relationships that could have appeared to influence the work reported in this paper.

DECLARATION OF GENERATIVE AI AND AI-ASSISTED TECHNOLOGIES IN THE WRITING PROCESS

During the preparation of this work, the authors used ChatGPT 5.1 in order to improve the language and readability of the manuscript. After using this tool/service, the authors reviewed and edited the content as needed and take full responsibility for the content of the publication.

FUNDING

This study was supported by funding from Pamukkale University (project number 2023HZDP006). This study is based on the doctoral thesis project of İsmail Hakkı Akbudak.

DATA AVAILABILITY

Data will be made available on request.

REFERENCES

1 Alfa RW, Park S, Skelly KR, Poffenberger G, Jain N, Gu X, et al. (2015). Suppression of insulin production and secretion by a decretin hormone. Cell Metab. **21**(2): 323–334. doi:10.1016/j.cmet.2015.01.004
2 Andreazzi AE, Scomparin DX, Mesquita FP, Balbo SL, Gravena C, De Oliveira JC, et al. (2009). Swimming exercise at weaning improves glycemic control and inhibits the onset of monosodium L-glutamate-obesity in mice. J Endocrinol. **201**(3): 351–359. doi:10.1677/JOE-08-0484
3 Austin C, Lo G, Nandha KA, Meleagros L, Bloom SR (1995). Cloning and characterization of the cDNA encoding the human neuromedin U (NmU) precursor: NmU expression in the human gastrointestinal tract. J Mol Endocrinol. **14**(2): 157–169. doi:10.1677/jme.0.0140157

4 Bernardis LL, Patterson BD (1968). Correlation between "Lee index" and carcass fat content in weanling and adult female rats with hypothalamic lesions. J Endocrinol. **40**(4): 527–528. doi:10.1677/joe.0.0400527

5 Boonnate P, Waraasawapati S, Hipkaeo W, Pethlert S, Sharma A, Selmi C, et al. (2015). Monosodium glutamate dietary consumption decreases pancreatic β-cell mass in adult Wistar rats. PLoS One. **10**(6): e0131595. doi:10.1371/journal.pone.0131595

6 Brosnan JT, Drewnowski A, Friedman MI (2014). Is there a relationship between dietary MSG and obesity in animals or humans? Amino Acids. **46**(9): 2075–2087. doi:10.1007/s00726-014-1771-6

7 Caponi PW, Lehnen AM, Pinto GH, Borges J, Markoski M, Machado UF, et al. (2013). Aerobic exercise training induces metabolic benefits in rats with metabolic syndrome independent of dietary changes. Clinics (Sao Paulo). **68**(7): 1010–1017. doi:10.6061/clinics/2013(07)22

8 Castrogiovanni D, Ongaro L, Zuburía G, Giovambattista A, Spinedi E (2015). Oral metformin treatment counteracts adipoinsular axis dysfunction in hypothalamic obese rats. Int Sch Res Notices. **2015**: 284042. doi:10.1155/2015/284042

9 Di Cairano ES, Davalli AM, Perego L, Sala S, Sacchi VF, La Rosa S, et al. (2011). The glial glutamate transporter 1 (GLT1) is expressed by pancreatic beta-cells and prevents glutamate-induced beta-cell death. J Biol Chem. **286**(16): 14007–14018. doi:10.1074/jbc.M110.200519

10 Dolnikoff M, Martín-Hidalgo A, Machado UF, Lima FB, Herrera E (2001). Decreased lipolysis and enhanced glycerol and glucose utilization by adipose tissue prior to development of obesity in monosodium glutamate (MSG) treated-rats. Int J Obes Relat Metab Disord. **25**(3): 426–433. doi:10.1038/sj.ijo.0801546

11 Ensho T, Maruyama K, Qattali AW, Yasuda M, Uemura R, Murakami N, et al. (2019). Comparison of glucose tolerance between wild-type mice and mice with double knockout of neuromedin U and neuromedin S. J Vet Med Sci. **81**(9): 1305–1312. doi:10.1292/jvms.19-0009

12 França LM, Coêlho CFF, Freitas LNC, Souza ILS, Chagas VT, Debbas V, et al. (2019). Syzygium cumini leaf extract reverts hypertriglyceridemia via downregulation of the hepatic XBP-1s/PDI/MTP axis in monosodium L-glutamate-induced obese rats. Oxid Med Cell Longev. **2019**: 9417498. doi:10.1155/2019/9417498

13 França LM, Freitas LN, Chagas VT, Coêlho CF, Barroso WA, Costa GC, et al. (2014). Mechanisms underlying hypertriglyceridemia in rats with monosodium L-glutamate-induced obesity: evidence of XBP-1/PDI/MTP axis activation. Biochem Biophys Res Commun. **443**(2): 725–730. doi:10.1016/j.bbrc.2013.12.031

14 Gaspar RS, Benevides RO, Fontelles JL, Vale CC, França LM, Barros Pde T, et al. (2016). Reproductive alterations in hyperinsulinemic but normoandrogenic MSG obese female rats. J Endocrinol. **229**(2): 61–72. doi:10.1530/JOE-15-0427

15 Hernández-Bautista RJ, Alarcón-Aguilar FJ, Del CE-VM, Almanza-Pérez JC, Merino-Aguilar H, Fainstein MK, et al. (2014). Biochemical alterations during the obese-aging process in female and male monosodium glutamate (MSG)-treated mice. Int J Mol Sci. **15**(7): 11473–11494. doi:10.3390/ijms150711473

16 Husarova V, Ostatnikova D (2013). Monosodium glutamate toxic effects and their implications for human intake: a review. J Med Res. **2013**: 460975. doi:10.5171/2013.608765

17 Leguisamo NM, Lehnen AM, Machado UF, Okamoto MM, Markoski MM, Pinto GH, et al. (2012). GLUT4 content decreases along with insulin resistance and high levels of inflammatory markers in rats with metabolic syndrome. Cardiovasc Diabetol. **11**: 100. doi:10.1186/1475-2840-11-100

18 Lehnen AM, Leguisamo NM, Casali KR, Schaan BD (2013). Progressive cardiovascular autonomic dysfunction in rats with evolving metabolic syndrome. Auton Neurosci. **176**(1-2): 64–69. doi:10.1016/j.autneu.2013.02.010

19 Maiter D, Underwood LE, Martin JB, Koenig JI (1991). Neonatal treatment with monosodium glutamate: effects of prolonged growth hormone (GH)-releasing hormone deficiency on pulsatile GH secretion and growth in female rats. Endocrinology. **128**(2): 1100–1106. doi:10.1210/endo-128-2-1100

20 Nagata M, Suzuki W, Iizuka S, Tabuchi M, Maruyama H, Takeda S, et al. (2006). Type 2 diabetes mellitus in obese mouse model induced by monosodium glutamate. Exp Anim. **55**(2): 109–115. doi:10.1538/expanim.55.109

21 Nagy C, Einwallner E (2018). Study of in vivo glucose metabolism in high-fat diet-fed mice using oral glucose tolerance test (OGTT) and insulin tolerance test (ITT). J Vis Exp. **131**: e56672. doi:10.3791/56672

22 Nakayama D, Magami Y, Azuma T, Inokuchi H, Furukawa M, Ohyashiki J, et al. (2003). Turnover of acinar and islet cells in the pancreas of monosodium glutamate-treated obese mice. Obes Res. **11**(1): 87–94. doi:10.1038/oby.2003.14

23 Olney JW (1969). Brain lesions, obesity, and other disturbances in mice treated with monosodium glutamate. Science. **164**(3880): 719–721. doi:10.1126/science.164.3880.719

24 Peier AM, Desai K, Hubert J, Du X, Yang L, Qian Y, et al. (2011). Effects of peripherally administered neuromedin U on energy and glucose homeostasis. Endocrinology. **152**(7): 2644–2654. doi:10.1210/en.2011-0155

25 Pelantová H, Bártová S, Anýž J, Holubová M, Železná B, Maletínská L, et al. (2016). Metabolomic profiling of urinary changes in mice with monosodium glutamate-induced obesity. Anal Bioanal Chem. **408**(2): 567–578. doi:10.1007/s00216-015-9167-4

26 Rogers P, Webb GP (1980). Estimation of body fat in normal and obese mice. Br J Nutr. **43**(1): 83–86. doi:10.1079/bjn19800064

27 Rosa DD, Grześkowiak ŁM, Ferreira CL, Fonseca AC, Reis SA, Dias MM, et al. (2016). Kefir reduces insulin resistance and inflammatory cytokine expression in an animal model of metabolic syndrome. Food Funct. **7**(8): 3390–3401. doi:10.1039/c6fo00290e

28 Sanches JR, França LM, Chagas VT, Gaspar RS, Dos Santos KA, Gonçalves LM, et al. (2016). Polyphenol-rich extract of Syzygium cumini leaf dually improves peripheral insulin sensitivity and pancreatic islet function in monosodium L-glutamate-induced obese rats. Front Pharmacol. **7**: 48. doi:10.3389/fphar.2016.00048

29 Teranishi H, Hanada R (2021). Neuromedin U, a key molecule in metabolic disorders. Int J Mol Sci. **22**(8): 4148. doi:10.3390/ijms22084148

30 Tunc-Ata M, Altintas F, Senol H, Nizamoglu E, Kucukatay V (2021). Ileal interposition improves metabolic syndrome parameters in a rat model of metabolic syndrome induced by monosodium glutamate. Life Sci. **266**: 118846. doi:10.1016/j.lfs.2020.118846

31 Windeløv JA, Pedersen J, Holst JJ (2016). Use of anesthesia dramatically alters the oral glucose tolerance and insulin secretion in C57Bl/6 mice. Physiol Rep. **4**(11): e12824. doi:10.14814/phy2.12824

32 Yin GS, Lin SD, Xu DC, Sun RQ, Lin K, Lin CJ (2013). Handle region peptide ameliorating insulin resistance but not β cell functions in male rats neonatally treated with sodium L-glutamate. Int J Endocrinol. **2013**: 493828. doi:10.1155/2013/493828

33 Zhang W, Sakoda H, Miura A, Shimizu K, Mori K, Miyazato M, et al. (2017). Neuromedin U suppresses glucose-stimulated insulin secretion in pancreatic β cells. Biochem Biophys Res Commun. **493**(1): 677–683. doi:10.1016/j.bbrc.2017.08.092

34 Zuurbier CJ, Keijzers PJ, Koeman A, Van Wezel HB, Hollmann MW (2008). Anesthesia's effects on plasma glucose and insulin and cardiac hexokinase at similar hemodynamics and without major surgical stress in fed rats. Anesth Analg. **106**(1): 135–142. doi:10.1213/01.ane.0000287686.95822.9f

Copyright © 2026 Neuroendocrinology Letters ISSN 0172–780X • **www.nel.edu**